Mon. Not. R. Astron. Soc. **000**, 1–11 (2014) Printed 8 December 2014 (MN LATEX style file v2.2)

Hybrid C-O-Ne white dwarfs as progenitors of type Ia supernovae: dependence on Urca process and mixing assumptions

arXiv:1407.0248v2 [astro-ph.SR] 5 Dec 2014

P. A. Denissenkov[1,4,9⋆], J. W. Truran[2,4,9], F. Herwig[1,4,9], S. Jones[1,5,9], B. Paxton[3], K. Nomoto[6,10], T. Suzuki[7] and H. Toki[8]

[1] *Department of Physics & Astronomy, University of Victoria, P.O. Box 1700, STN CSC, Victoria, B.C., V8W 2Y2, Canada*
[2] *Department of Astronomy and Astrophysics, and Enrico Fermi Institute, University of Chicago, Chicago, IL 60637 USA*
[3] *Kavli Institute for Theoretical Physics and Department of Physics, Kohn Hall, University of California, Santa Barbara, CA 93106, USA*
[4] *The Joint Institute for Nuclear Astrophysics, Notre Dame, IN 46556, USA*
[5] *Astrophysics Group, Research Institute for the Environment, Physical Sciences and Applied Mathematics, Keele University, Keele, Staffordshire ST5 5BG*
[6] *Kavli Institute for Physics and Mathematics of the Universe (WPI), The University of Tokyo, Kashiwa, Chiba 277-8583, Japan*
[7] *Department of Physics, College of Humanities and Sciences, Nihon University, Sakurajosui 3-25-40, Setagaya-ku, Tokyo 156-8550, Japan*
[8] *Research Center for Nuclear Physics, (RCNP), Osaka University, Ibaraki, Osaka 567-0047, Japan*
[9] *NuGrid collaboration*
[10] *Hamamatsu Professor*

Accepted 2014 December 31. Received 2014 December 31; in original form 2014 December 31

ABSTRACT

When carbon is ignited off-centre in a CO core of a super-AGB star, its burning in a convective shell tends to propagate to the centre. Whether the C flame will actually be able to reach the centre depends on the efficiency of extra mixing beneath the C convective shell. Whereas thermohaline mixing is too inefficient to interfere with the C-flame propagation, convective boundary mixing can prevent the C burning from reaching the centre. As a result, a C-O-Ne white dwarf (WD) is formed, after the star has lost its envelope. Such a "hybrid" WD has a small CO core surrounded by a thick ONe zone. In our 1D stellar evolution computations, the hybrid WD is allowed to accrete C-rich material, as if it were in a close binary system and accreted H-rich material from its companion with a sufficiently high rate at which the accreted H would be processed into He under stationary conditions, assuming that He could then be transformed into C. When the mass of the accreting WD approaches the Chandrasekhar limit, we find a series of convective Urca shell flashes associated with high abundances of ^{23}Na and ^{25}Mg. They are followed by off-centre C ignition leading to convection that occupies almost the entire star. To model the Urca processes, we use the most recent well-resolved data for their reaction and neutrino-energy loss rates. Because of the emphasized uncertainty of the convective Urca process in our hybrid WD models of SN Ia progenitors, we consider a number of their potentially possible alternative instances for different mixing assumptions, all of which reach a phase of explosive C ignition, either off or in the centre. Our hybrid SN Ia progenitor models have much lower C to O abundance ratios at the moment of the explosive C ignition than their pure CO counterparts, which may explain the observed diversity of the SNe Ia.

Key words: stars: evolution — stars: interiors — white dwarfs — supernovae: general — methods: numerical

1 INTRODUCTION

Type Ia supernovae (hereafter, SNe Ia) are thermonuclear explosions of carbon-oxygen white dwarfs (CO WDs) (Hillebrandt & Niemeyer 2000). When the mass of a CO WD

⋆ E-mail: pavelden@uvic.ca.

approaches the Chandrasekhar limit $M_{\rm Ch} \approx 1.39\,M_\odot$ and, as a consequence, the star is about to lose its hydrostatic equilibrium, C burning near the centre enters the phase of a thermonuclear runaway leading to an SN Ia explosion. SNe Ia are important objects because they are the main producers of iron peak elements and also because of their single-parameter light curves (Phillips 1993) that allow to measure their peak luminosities with a high precision. The latter property of SNe Ia has made them a standard candle in extragalactic astronomy, which was used to discover the accelerating expansion of the Universe (Riess et al. 1998; Perlmutter et al. 1999).

CO WDs are the cores of asymptotic giant branch (AGB) stars that get exposed after their parent stars have lost their envelopes via stellar winds or unstable mass transfers in binary systems. Masses of newly born CO WDs range from $\sim 0.6\,M_\odot$ to $\sim 1\,M_\odot$, therefore the CO WDs need to accrete some extra mass for them to reach $M_{\rm Ch}$. For SNe Ia, such accretion has been proposed to occur either through a single degenerate (SD) channel, when the extra mass is provided by WD's main sequence, subgiant, or red giant companion, or through a double degenerate (DD) channel, when two CO WDs with a total mass larger than $M_{\rm Ch}$ merge (Wang & Han 2012). There also exists a possibility that a CO WD with a mass less than $M_{\rm Ch}$ accretes He from its binary companion, which became a He star earlier, until the accreted layer of $\sim 0.04-0.08\,M_\odot$ of He detonates near its base causing a detonation of the underlying CO WD (Nomoto 1982a; Iben & Tutukov 1991; Woosley & Weaver 1994; Shen & Bildsten 2009).

There is an upper limit $M_{\rm u}$ for the initial mass of a star $M_{\rm i}$, such that in a star with $M_{\rm i} > M_{\rm u}$ carbon is ignited off-centre in the CO core on the AGB. Such stars are called super AGB stars. If no other mixing is present in the CO core, except convection driven by the C burning, then the C flame propagates all the way down to the centre resulting in the formation of an oxygen-neon core that will become an ONe WD after the envelope is lost. Therefore, only the stars with $M_{\rm i} < M_{\rm u}$ are usually considered to be able to leave remnants that may lead to SN Ia explosions, provided that they initially reside in binary systems with parameters suitable for the SD or DD channel. A theoretical value of $M_{\rm u}$ depends on various model parameters and assumptions, such as the metallicity, or the heavy-element mass fraction Z (Becker & Iben 1979), the adopted carbon burning rate, that is still very uncertain (Chen et al. 2014), as well as on the extent of convective boundary mixing outside the H and He convective cores and stellar rotation, both of which work towards increasing the final mass of the H-free core, hence decreasing $M_{\rm u}$.

There are several potential mixing mechanisms that can operate below the C-burning convective shell in the CO core. Two of them, thermohaline mixing and convective boundary mixing (CBM), have been studied by Denissenkov et al. (2013) using the most recent estimates of their efficiencies in stars obtained from multi-dimensional numerical simulations. It has been shown that thermohaline mixing cannot interfere with the C-flame propagation, in spite of quite a strong positive mean molecular weight gradient produced by the off-centre C burning, because of a small aspect ratio of participating fluid parcels ("salt fingers"). On the other hand, even a small amount of CBM turns out to be sufficient to remove physical conditions required for the C-flame to propagate all the way to the centre. As a result, the C flame stalls at some distance from the centre, leaving below a small core of unburnt C and O. The works of Denissenkov et al. (2013) and Chen et al. (2014) have introduced a new class of hybrid cores of super-AGB stars and their corresponding WDs that consist of small CO cores surrounded by thick ONe zones.

In this paper, we aim to find out if the hybrid C-O-Ne WDs can be progenitors of SNe Ia. In the case of a positive answer, this will slightly increase the upper limit for the initial mass of the star that can potentially end up as an SN Ia, from $M_{\rm u}$ to $M_{\rm u} + \Delta M_{\rm u}^{\rm hy}$, assuming that stars with $M_{\rm i} < M_{\rm u}$ produce pure CO WDs, while those with $M_{\rm i} > M_{\rm u} + \Delta M_{\rm u}^{\rm hy}$ give birth to pure ONe WDs. What is probably even more important is that the hybrid C-O-Ne WDs may become progenitors of unusual SNe Ia, thus contributing to their diversity, because chemical and thermal structures of the hybrid SN Ia progenitors are expected to be very different from those of the standard CO progenitors. In particular, we anticipate that Urca processes will be essential for the hybrid SN Ia progenitors, because C burning usually results in a relatively high abundance of ^{23}Na that forms an Urca pair with ^{23}Ne.

The structure of our paper is simple. In § 2, we describe how we calculate our models, including our treatment of the Urca processes. Our results are presented in § 3, which is followed by the final section where we discuss the results and make conclusions.

2 COMPUTATIONAL METHOD

In this section, we describe the computer code and methods that we have used to calculate our SN Ia progenitor models and we discuss our treatment of the mass accretion and Urca processes.

2.1 Computer code

We have used the revision 5329 of MESA (the Modules for Experiments in Stellar Astrophysics) to prepare models of CO, ONe and hybrid C-O-Ne WDs and to compute their evolution, driven by accretion, towards the beginning of SN Ia explosion or electron-capture induced collapse. MESA[1] is a suite of an open source modern stellar evolution code and related modules (Paxton et al. 2011, 2013). We employ the same MESA equation of state, opacities and reaction rates as in the work of Denissenkov et al. (2013). Our nuclear network is similar to the largest one (`nova.net`) with 77 isotopes from H to ^{40}Ca coupled by 442 reactions that was used by Denissenkov et al. (2014) to prepare WD models for their simulations of ONe nova outbursts, except that it has been extended to 87 isotopes and 500 reactions to include the MESA electron capture network and a new Urca network that become important at very high densities. The Urca network makes use of the well resolved tables of reaction and neutrino-loss rates for Urca pairs with atomic numbers $A = 23$, 25 and 27 calculated by Toki et al. (2013).

[1] `http://mesa.sourceforge.net`

A detailed discussion of the new Urca rates and their comparison with the old data of Oda et al. (1994) can be found in the paper of Jones et al. (2013).

Our stellar evolution models have $Z = 0.014$ and the initial hydrogen mass fraction $X = 0.70$. In convective zones, we use the mixing length theory (MLT) of Cox & Giuli (Weiss et al. 2004) with a solar calibrated ratio $\alpha_{\rm MLT} = \Lambda/\lambda_P = 1.91$ of the mixing length to the pressure scale height. The CBM outside a convective zone is modeled with the diffusion coefficient

$$D_{\rm CBM}(r) = D_{\rm MLT}(r_0)\exp\left(-\frac{|r-r_0|}{f\lambda_P}\right), \quad (1)$$

where $D_{\rm MLT}(r_0) = (\Lambda v_{\rm conv})/3$ is a value of the convective diffusion coefficient at a distance $f\lambda_P$ from the Schwarzschild boundary inside the convective zone calculated using local MLT values of Λ and convective velocity. Like Denissenkov et al. (2013) and Chen et al. (2014), we use the CBM parameter $f = 0.014$ for the H and He convective core boundaries, while we assume $f = 0.007$ for the stiffer boundaries of the He and C convective shells.

To create a set of WDs with different initial masses and chemical structures, we use the new MESA test suite case `make_co_wd`. We calculate the evolution of a star from the pre-main sequence to the end of core C burning in super-AGB stars or to the first He-shell thermal pulse in AGB stars that do not ignite C (the dark blue segment of the track in Fig. 1). Then, we artificially increase the mass-loss rate (the green segment), while using the new MLT++ prescription for radiation-dominated envelopes with super-adiabatic convection to keep calculation timesteps reasonably large (Paxton et al. 2013). After that, we allow our model to lose the rest of its envelope until neither H nor He is left at its surface (the red segment). The naked WD is then cooled down to a specified central temperature $T_{\rm c}$ (the light blue segment). The resulting mass fraction profiles of ^{12}C in the cores of AGB and super-AGB stars immediately before the mass-loss rate is increased are shown in Fig. 3. These include pure CO and hybrid C-O-Ne cores.

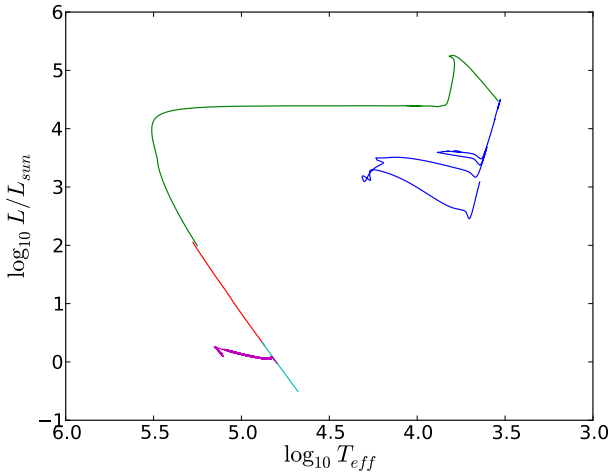

Figure 1. Evolutionary track of the star with $M_{\rm i} = 6.3\,M_\odot$ calculated from the pre-main sequence through to the WD cooling sequence (the dark blue, green, red and light blue segments) using the MESA test suite case `make_co_wd`. After that, the WD is allowed to accrete C-rich material until its mass approaches the Chandrasekhar limit and, as a consequence, C is ignited in the centre and then its burning enters the phase of thermonuclear runaway (the magenta segment).

2.2 Mass accretion

In the SD channel, a WD accretes H-rich material from its binary companion. There is a lower limit $\dot{M}_{\rm stable}$ for the mass accretion rate $\dot{M}_{\rm acc}$, such that only for $\dot{M}_{\rm acc} > \dot{M}_{\rm stable}$ the accreted H is transformed into He in a stable nuclear burning (Nomoto 1982b). Lower accretion rates lead to H shell flashes followed by ejecta of processed material, resulting in events known as nova outbursts (e.g., Denissenkov et al. 2014). Spectroscopic observations of ejecta of classical novae reveal that most of them are strongly enriched in heavy elements, which is interpreted as a result of mixing with underlying WDs (e.g., Gehrz et al. 1998). Therefore, masses of WDs in the classical nova systems are unlikely to increase with time. However, this is probably not true for the recurrent nova systems, in which WDs with masses close to the Chandrasekhar limit accrete H with rates close to $\dot{M}_{\rm stable}$. This makes them good candidates for the SD channel of SN Ia progenitors (Wolf et al. 2013; Tang et al. 2014).

There is also an upper limit $\dot{M}_{\rm RG}$, such that H accreted by a WD with a rate $\dot{M}_{\rm acc} > \dot{M}_{\rm RG}$ cannot be transformed into He fast enough to avoid its accumulation around the WD. This leads to expansion of the accreted H-rich envelope, so that the accreting star tends to become a red giant. To expand the narrow range of $\dot{M}_{\rm acc}$ suitable for the SD channel, Hachisu, Kato & Nomoto (1996) and Ma et al. (2013) proposed to replace the red-giant regime with the thick-wind and super-Eddington regimes, respectively, in either of which the excess of mass that is accreted with $\dot{M}_{\rm acc} > \dot{M}_{\rm RG}$ but not processed in the H-shell burning is blown off the binary system.

To find out if the hybrid C-O-Ne WDs can be progenitors of SNe Ia, we allow our hybrid WD models to accrete material with chemical composition identical to that of their surface layers. Because our hybrid WD models have CO-rich surface buffer zones (Fig. 3), their surface chemical composition corresponds to that of products of the He shell burning, and so does the composition of the accreted material. In this case, we do not have problems with the H burning and He shell flashes in the accreted envelope, like those encountered by Cassisi, Iben & Tornambè (1998). Therefore, we use accretion rates that are not necessarily always in the range $\dot{M}_{\rm stable} < \dot{M}_{\rm acc} < \dot{M}_{\rm RG}$, but with which we can relatively quickly calculate the evolution of our accreting WDs till the beginning of an SN Ia explosion. With this simple method, we can neglect all the uncertainties associated with the accretion of H-rich material onto a WD in the SD channel, such as the H and He retention efficiencies (Bours, Toonen & Nelemans 2013), while trying to find out if C in our hybrid WD models will eventually ignite and its burning enter the phase of thermonuclear runaway when their masses approach the Chandrasekhar limit. By the same reason, we do not make an evolutionary motivated choice of the initial central temperatures of our WDs when the accretion begins.

For a more systematic study of the evolution of pure CO WDs from the onset of accretion to the explosive C ignition for a set of $T_{\rm c}$ and $\dot{M}_{\rm acc}$ values suitable for the SD channel,

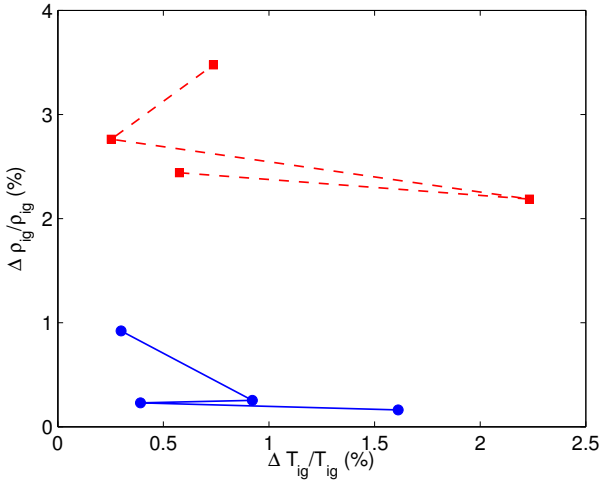

Figure 2. Relative differences in temperature and density at the explosive C ignition between two sets of CO WD models accreting CO-rich material, according to data from Tables 1 and 2 of Chen, Han & Meng (2014). The first set, like our models, neglects both H and He burning, whereas in the second set their energy generation rates are approximated by an extra source of 10^5erg g^{-1}s^{-1} included in the outermost zones of the accreting WD models. The data are plotted for the $1.0M_\odot$ WD model with the cooling times (when the accretion begins) ranging from 0.01 to 0.2 Gyr (solid blue curves corresponding to central C ignition) and from 0.4 to 1.5 Gyr (dashed red curves for off-centre C ignition).

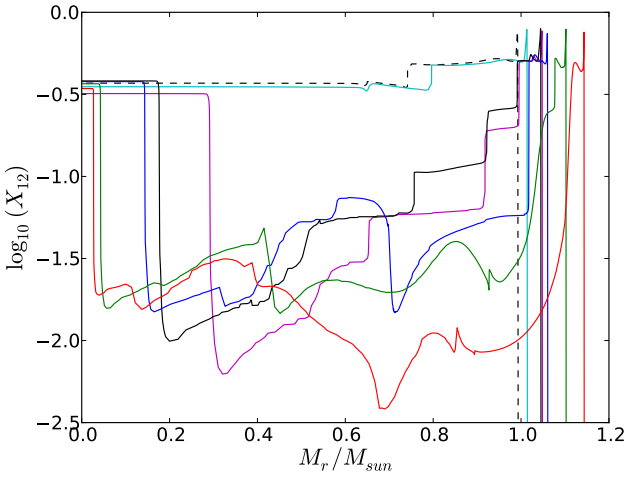

Figure 3. Mass fraction profiles of ^{12}C at the end of carbon burning in hybrid C-O-Ne cores of super-AGB stars. A value of $f = 0.014$ was used to model convective boundary mixing (CBM) at all convective boundaries, except the stiffer boundaries of the He and C convective shells, where a value of $f = 0.007$ was assumed. The initial masses of the AGB stars are $6.3\,M_\odot$ (dashed black curve), $6.4\,M_\odot$ (cyan curve), $6.5\,M_\odot$ (magenta curve), $6.8\,M_\odot$ (solid black curve), $6.9\,M_\odot$ (blue curve), $7.1\,M_\odot$ (green curve), and $7.3\,M_\odot$ (red curve). In the first two models, C has not ignited in the CO cores.

the interested reader is referred to the recent study by Chen, Han & Meng (2014), who also used MESA and assumed the accretion of CO-rich material, although they did not include Urca reactions.

In our considered cases, the luminosity of an accreting WD is actually determined by a release of the gravitational energy of accreted material as well as by the stationary H burning alternating with He shell flashes. Our neglect of the H and He thermonuclear energy sources results in a relatively low luminosity of our accreting WD model (e.g., Fig. 1). To estimate possible effects of this neglect on the SNIa progenitor models, Chen, Han & Meng (2014) have included an extra source with the energy generation rate of 10^5erg g^{-1}s^{-1} in the outermost zones of their WD models that, like our models, accrete CO-rich material. Fig. 2, in which we have used data from Tables 1 and 2 of the cited paper, shows that the relative differences in temperature and density at the explosive C ignition between the two sets of models, the one with and the other without the extra source simulating the energy generation in the H and He burning, do not exceed a few percent even for WD models with very long cooling times in which C is ignited off-centre.

For the accreted material, the MESA stellar evolution code uses the thin-shell radiation calculation of the gravitational energy generation rate (Equation 18 in Paxton et al. 2013). It is obtained under the realistic assumption that the thermal timescale is much shorter than the local accretion time in the outermost layers, therefore the accreted material adjusts its temperature to a value nedded to transport the stellar luminosity from the underlying layers out.

2.3 The Urca process uncertainty

The Urca process is an electron capture reaction that transforms a mother nucleus M into a daughter nucleus D followed by a beta decay of D back to M. During this process, a neutrino and an anti-neutrino are emitted that escape the star carrying away some energy, which leads to a local cooling (Gamow & Schoenberg 1941). The Urca process starts when the electron chemical potential μ_e exceeds a threshold value μ_{th} for the corresponding Urca pair M/D. In the electron degenerate matter, μ_e mainly depends on the density ρ, therefore the condition for the occurrence of the Urca process is $\rho > \rho_{th}$. In compact stars with high central densities ρ_c, like the WDs with masses approaching the Chandrasekhar limit, only those Urca pairs are important that have relatively high abundances of M nuclei and for which $\rho_c > \rho_{th}$. In our case, these are the pairs ^{25}Mg/^{25}Na with $\rho_{th} = 1.29 \times 10^9$ g cm^{-3} ($\log_{10}\rho_{th} = 9.11$) and, especially, ^{23}Na/^{23}Ne with $\rho_{th} = 1.66 \times 10^9$ g cm^{-3} ($\log_{10}\rho_{th} = 9.22$)[2]. The mass fraction profiles of ^{23}Na and ^{25}Mg in the cores of three stars from Fig. 3 are shown in Fig. 4. The abundances of ^{23}Na are much larger in the super-AGB stars because of C burning in the reaction ^{12}C+^{12}C$\rightarrow^{23}$Na+^{1}H.

Using the electron-capture rate λ^+, beta-decay rate λ^- and their corresponding neutrino-energy loss rates $L^\pm$ per one M and D nucleus from the tables of Toki et al. (2013), we can calculate a total rate of change of thermal energy in the so-called "Urca shell", where $\rho = \rho_{th}$. Per unit volume,

[2] The density estimates are obtained for the electron number fraction $Y_e = 0.5$

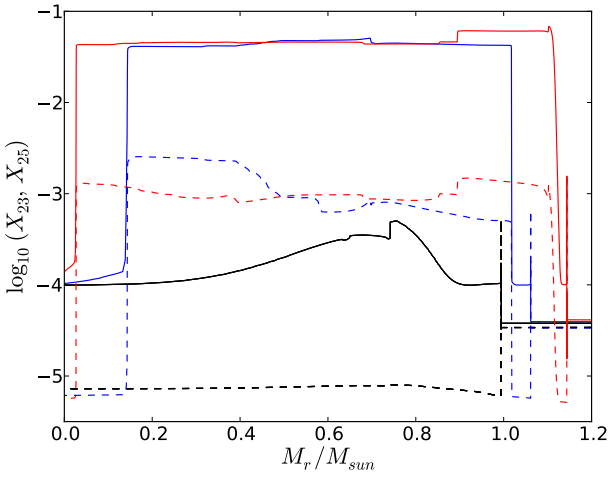

Figure 4. Mass fraction profiles of ^{23}Na (solid curves) and ^{25}Mg (dashed curves) in the CO core of the AGB star with $M_{\rm i} = 6.3\,M_{\odot}$ (black curves) after the first He-shell thermal pulse, and in the hybrid C-O-Ne cores of the super-AGB stars with the initial masses $6.9\,M_{\odot}$ (blue curves) and $7.3\,M_{\odot}$ (red curves) at the end of C burning.

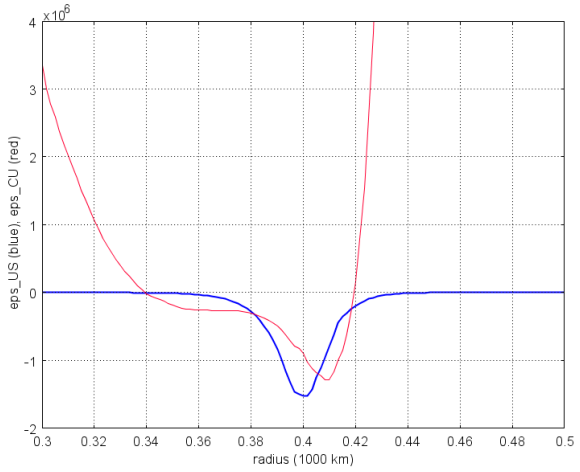

Figure 5. The Urca cooling caused by neutrino and antineutrino escaping from the Urca shell (the blue curve) and the combined Urca cooling and heating (the red curve), the latter caused by non-equilibrium electron captures and beta decays around the Urca shell in the presence of convective mixing in the CO WD with $M_{\rm i} = 6.3\,M_{\odot}$. Both quantities are given in erg cm^{-3} s^{-1}.

it is equal to

$$\varepsilon_{\rm U} = -\delta\mu\,\frac{d\,n_{\rm M}}{dt} - L^{+}n_{\rm M} - L^{-}n_{\rm D}, \tag{2}$$

where $n_{\rm M}$ and $n_{\rm D}$ are number densities of the M and D nuclei,

$$\frac{d\,n_{\rm M}}{dt} = -\lambda^{+}n_{\rm M} + \lambda^{-}n_{\rm D}, \tag{3}$$

and

$$\delta\mu = \mu_{\rm e} - \mu_{\rm th} = (\mu_{\rm e} - V_{\rm s}) - (Q - \delta Q) - m_{\rm e}c^2. \tag{4}$$

The screening corrections to the electron potential and reaction Q-value, $V_{\rm s}$ and δQ, used in the last equation are also provided by the tables. Note that δQ is negative for beta decays and positive for e-captures.

Introducing the total number density of the Urca pair nuclei $n_{\rm U} = n_{\rm M} + n_{\rm D}$, equation (2) can be rewritten in the following form:

$$\varepsilon_{\rm U} = Cn_{\rm U} + H(n_{\rm M} - n^{*}_{\rm M}), \tag{5}$$

where

$$n^{*}_{\rm M} = \frac{\lambda^{-}}{\lambda^{+} + \lambda^{-}}\,n_{\rm U} \tag{6}$$

is an equilibrium number density of the mother nuclei, while

$$C = -\frac{L^{+}\lambda^{-} + L^{-}\lambda^{+}}{\lambda^{+} + \lambda^{-}} \tag{7}$$

and

$$H = \delta\mu\,(\lambda^{+} + \lambda^{-}) - L^{+} + L^{-} \tag{8}$$

are the cooling and heating factors (Lesaffre, Podsiadlowski & Tout 2005). Equation (5) shows that the Urca process can cool the star down only in the vicinity of the Urca shell, where the first term is negative and the second term is close to zero. However, if the Urca shell is involved in convective mixing that redistributes the Urca nuclei accross the Urca shell, then the second term turns out to be always positive and it starts to dominate over the cooling term at some distance from the Urca shell (Fig. 5). Therefore, such a "convective Urca process" should contribute to both cooling near the Urca shell and heating outside it (Bruenn 1973).

Although MESA does take into account the Urca energy loss/generation rate, e.g. as given by equation (5), it does not modify the MLT equations correspondingly, ignoring the fact that in the convective Urca process the kinetic energy of convective motion serves as a source for both Urca cooling and heating (Bisnovatyi-Kogan 2001). This means that in MESA the Urca process can affect convection only through changes of star's thermal structure.

Since the first discussion of convective Urca process by Paczyński (1972), there has been found no satisfactory solution of this problem. The proposed solutions contradict each other, because some of them predict that the convective Urca process should stabilize C burning, thus allowing the accreting WD to avoid the SN Ia explosion (Paczyński 1972; Iben 1982; Barkat & Wheeler 1990), while the others claim that it should rather destabilize C burning sooner or later, thus leading to an earlier or delayed thermonuclear runaway (Bruenn 1973; Couch & Arnett 1975; Mochkovitch 1996; Stein, Barkat & Wheeler 1999).

The convective Urca process should probably decrease the volume occupied by convection that is driven by C burning during the pre-explosion simmering phase (Lesaffre, Podsiadlowski & Tout 2005; Stein & Wheeler 2006). However, we believe that a final solution of the convective Urca problem and, in particular, a reliable estimate of the limit imposed by it on the size of the C convective core can be obtained only in reactive-convective 3D hydrodynamical simulations. For example, these kinds of simulations of H entrainment by He-shell flash convection in the post-AGB star Sakurai's object has recently revealed a very interesting and complex mixing behaviour which could never be predicted by a mixing length theory (Herwig et al. 2014). Until such simulations are done

for the convective Urca process, we choose to present the results of our calculations of SN Ia progenitor models for a number of different mixing assumptions that are supposed to mimic potentially possible outcomes of the interaction of convection and Urca reactions.

3 RESULTS

We present the results only for three of our accreting WD models: the first one is the pure CO WD with the initial mass $M_{\rm i} = 6.3\,M_\odot$ (the dashed black curve in Fig. 3), the second is the hybrid WD with $M_{\rm i} = 7.3\,M_\odot$ that has a very small CO core left at the end of C burning (the red curve in Fig. 3), and the third is the hybrid WD with $M_{\rm i} = 6.9\,M_\odot$ that has a relatively large CO core (the blue curve in Fig. 3). The first model is a standard one for the SD channel of SN Ia progenitors. We include it for the completeness of our study. The second model is close to the pure ONe WDs, therefore we expect that it will end up as an electron-capture supernova (ECSN) (Jones et al. 2013). The abundance profiles of the Urca mother nuclei ^{23}Na and ^{25}Mg for these models are plotted in Fig. 4.

3.1 The pure CO WD model with $M_{\rm i} = 6.3\,M_\odot$

The evolution of this WD model towards the explosive C ignition has been calculated relatively quickly with the mass accretion rate $\dot{M}_{\rm acc} = 10^{-8}\,M_\odot\,{\rm yr}^{-1}$. It is an order of magnitude lower than the corresponding value of $\dot{M}_{\rm stable}$ (Hachisu, Kato & Nomoto 1996; Nomoto et al. 2007; Ma et al. 2013), but, as we explained before, a choice of evolutionary motivated values of $\dot{M}_{\rm acc}$ and $T_{\rm c}$ is out of the scope of the present study. In spite of this, our calculated central temperature and density at the explosive C ignition near the right end of the black curve in Fig. 6 are very close to their corresponding values $\log_{10} T_{\rm c} = 9.0$ and $\log_{10} \rho_{\rm c} = 9.4$ reported by Chen, Han & Meng (2014), who chose the initial model parameters more carefully. Our final WD mass $M_{\rm WD} = 1.386\,M_\odot$ is also close to their value of $1.387\,M_\odot$. We have compared their final WD parameters with those obtained by us for the case without Urca processes ("no Urca") because Chen, Han & Meng (2014) did not include any Urca reactions.

The red curve in Fig. 6 shows the evolution of $T_{\rm c}$ and $\rho_{\rm c}$ for our standard case, when the Urca reactions are included using the new well-resolved tables of Toki et al. (2013). The two steps near the left ends of all the curves that include the Urca processes are produced by sudden cooling at the centre happening when the increasing central density first exceeds the Urca threshold density for ^{25}Mg and then the one for ^{23}Na. Note that the red and black curves would be indistinguishable if we used the old Urca reaction data of Oda et al. (1994).

To model the convective Urca process, Lesaffre, Podsiadlowski & Tout (2005) developed a new two-stream formalism. For stationary conditions, they found strong reductions of the convective velocity by the Urca process when the mass fraction of ^{23}Na was increasing from $X_{23} = 10^{-9}$ to $X_{23} = 10^{-3}$. Similarly, in their 2D hydrodynamical simulations of the convective Urca process, that they called "an indicative but still qualitative study" because of artificially increased reaction rates, Stein & Wheeler (2006) observed a

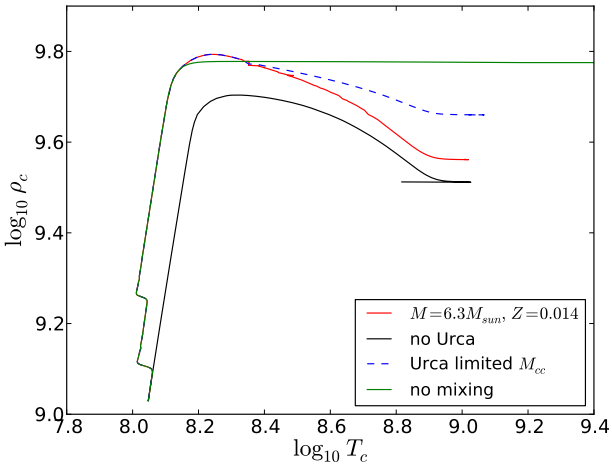

Figure 6. Red curve shows the evolution of central temperature and density resulting from the accretion of C-rich surface-composition material onto the pure CO white dwarf with the rate of $10^{-8}\,M_\odot\,{\rm yr}^{-1}$. The initial mass of the star is $6.3\,M_\odot$ (the dashed black curve in Fig. 3). Other calculations did not include the Urca reactions ("no Urca"), assumed that the boundary of the C-burning convective core $M_{\rm cc}$ is located at the ^{23}Na/^{23}Ne Urca shell ("Urca limited $M_{\rm cc}$), or completely turned off convective mixing ("no mixing"). In the third and fourth cases, the density of explosive C ignition is higher than in the first two cases.

confinement of the C convective core by the ^{23}Na/^{23}Ne Urca shell for $X_{23} = 4 \times 10^{-4}$. Taking these results into account and also the fact that our hybrid WD models have very large abundances of ^{23}Na (Fig. 4), we consider as potentially possible outcomes of the convective Urca process cases in which it either limits the mass of the C convective core $M_{\rm cc}$ by a mass coordinate where the ^{23}Na/^{23}Ne Urca shell is located or completely suppresses convective mixing. For our mixing assumptions corresponding to these two cases that we call "Urca limited $M_{\rm cc}$" and "no mixing", the resulting $T_{\rm c}$ - $\rho_{\rm c}$ trajectories are also plotted in Fig. 6.

3.2 The hybrid WD model with $M_{\rm i} = 7.3\,M_\odot$ that has a small CO core

When C is first ignited in the centre of this model, convection driven by the C burning dilutes the high C abundance in the small core with the low C abundance in the surrounding ONe zone (the red curve in Fig. 3). The diluted C abundance $X_{12} \approx 0.02$ turns out to be too low for the C burning to compete with the neutrino cooling and, as a result, the central temperature rapidly decreases after its initial attempt to go up caused by the C ignition (the first zigzag at densities between $\log_{10} \rho_{\rm c} = 9$ and $\log_{10} \rho_{\rm c} = 9.5$ in Fig. 7). The continuing mass accretion with the rate $\dot{M}_{\rm acc} = 8 \times 10^{-7}\,M_\odot\,{\rm yr}^{-1}$, which is close to the upper limit $\dot{M}_{\rm RG}$, unless we account for the thick-wind and super-Eddington regimes (Hachisu, Kato & Nomoto 1996; Ma et al. 2013), leads to a further increase of the central density until it reaches a value at which electron-capture reactions become efficient (the second zigzag at $\log_{10} \rho_{\rm c} > 10$ in Fig. 7). Eventually, these reactions should induce a collapse of the star resulting in an

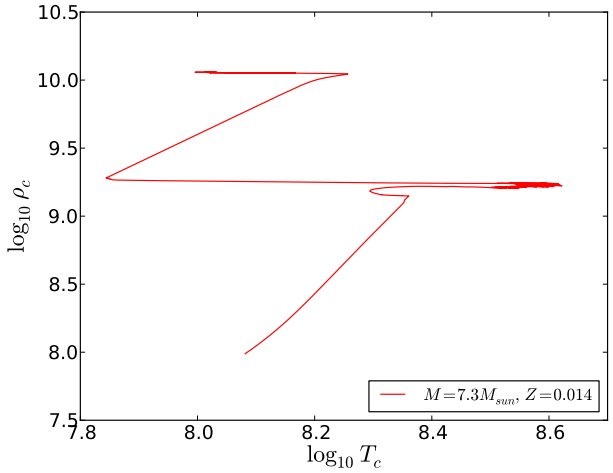

Figure 7. Same as in Fig. 6, but for the hybrid C-O-Ne white dwarf with $M_{\rm i} = 7.3\,M_{\odot}$ (the solid red curve in Fig. 3) and for the mass accretion rate of $8 \times 10^{-7}\,M_{\odot}\,{\rm yr}^{-1}$. In this case, C fails to ignite explosively because of its low abundance, and the star evolves towards electron-capture induced collapse.

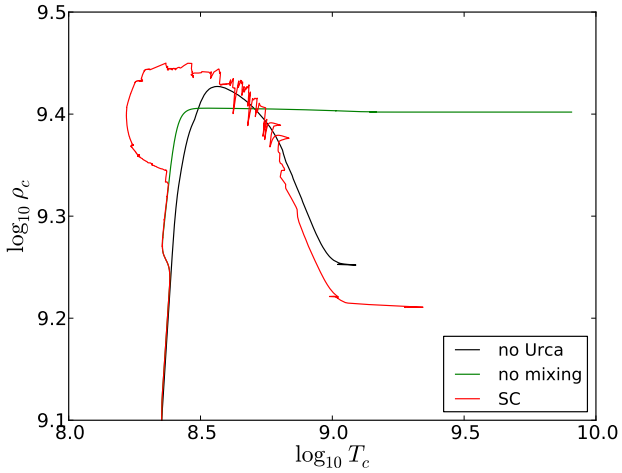

Figure 8. Same as in Fig. 6, but for the hybrid C-O-Ne white dwarf with $M_{\rm i} = 6.9\,M_{\odot}$ (the solid blue curve in Fig. 3) and for the mass accretion rate of $8 \times 10^{-7}\,M_{\odot}\,{\rm yr}^{-1}$. In these three case, the explosive C ignition takes place in the centre.

ECSN, like in the cases of more massive pure ONe cores of super-AGB stars considered by Jones et al. (2013).

3.3 The hybrid WD model with $M_{\rm i} = 6.9\,M_{\odot}$ that has a relatively large CO core

This WD model is quite different from the previous two models. Indeed, on the one hand, it has a relatively large CO core (the blue curve in Fig. 3), so that even after the dilution of C from the core in the ONe zone its abundance may still be high enough for the C burning to compete with the neutrino cooling. On the other hand, ^{25}Mg and, especially, ^{23}Na have so high abundances outside the CO core in this model (the dashed and solid blue curves in Fig. 4) that it is difficult to make a prediction, based on our 1D stellar evolution calculations with the MLT prescription for convection, of how the convective Urca process will affect the model thermal and chemical structures. Therefore, until appropriate reactive-convective 3D hydrodynamical simulations of this process provide more realistic prescriptions for the modeling of its effects on the explosive C ignition in the CO and hybrid C-O-Ne WDs in 1D stellar evolution codes, we have nothing else but to consider a number of instances of this accreting WD model obtained for different assumptions about possible outcomes of the interaction between convective mixing and Urca reactions that might be suggested by such simulations in the future.

Like the previous hybrid model, this WD model accretes C-rich material with the rate $\dot{M}_{\rm acc} = 8 \times 10^{-7}\,M_{\odot}\,{\rm yr}^{-1}$. We start with the case without Urca reactions. Its corresponding WD's evolution on the $T_{\rm c}$ - $\rho_{\rm c}$ plane is shown with the black curve in Fig. 8, while its Kippenhahn diagram is plotted in Fig. 9b. Similar to Fig. 6, the green curve in Fig. 8 has been calculated for the case when all mixing is assumed to be suppressed by the Urca processes.

Our standard case with CBM produces a set of two black curves on the $T_{\rm c}$ - $\rho_{\rm c}$ plane in Fig. 10. The Urca process involving the ^{23}Na/^{23}Ne pair turns out to generate so efficient cooling in the centre of this hybrid WD model, when its mass approaches the Chandrasekhar limit, that the maximum temperature is reached and the explosive C ignition occurs off the centre, as shown with the solid black curve in Fig. 10 and in Fig. 9a. This shift of $T_{\rm max}$ from the centre to a point where $\rho < \rho_{\rm th}$ for the ^{23}Na/^{23}Ne Urca pair and where the Urca process can therefore not interfere with the C burning is facilitated by a series of convective Urca shell flashes near the centre. These flashes are seen in Fig. 9a and, especially, in the zoomed in version of this figure in Fig. 11, which uses the shades of blue to additionally show the positive energy generation rate. The convective shell flashes are caused by intermittent changes in the temperature profile taking place where the internal energy experiences local variations, as described by equation (5). However, given that both Urca cooling and heating should probably drain convective motion of its kinetic energy (Bisnovatyi-Kogan 2001), which is not taken into account in our MLT prescription for convection, these "convective Urca flashes" may simply be an artefact of our crude model. Their presence is not related to our using the CBM, because when we do not include the CBM they are still present (the case of "no CBM" in Fig. 10 and Fig. 9c). The addition of semiconvection (the case "CBM+SC"), following the prescription of Langer, El Eid & Fricke (1985) with the efficiency parameter $\alpha_{\rm sc} = 0.01$, does not change qualitatively their behaviour. The semiconvection may be important near the boundaries of convective Urca shells, because Urca reactions build a gradient of the mean molecular weight that opposes a convectively unstable temperature gradient (e.g. Lesaffre, Podsiadlowski & Tout 2005), although the CBM should dominate over semiconvection in regions where they are both present. Surprisingly, when we include only semiconvection ("SC") then $T_{\rm max}$ and the point of the explosive C ignition are not shifted from the centre (Fig. 9f), however we believe that the CBM should always be included as well. Finally, in the case of "Urca lim-

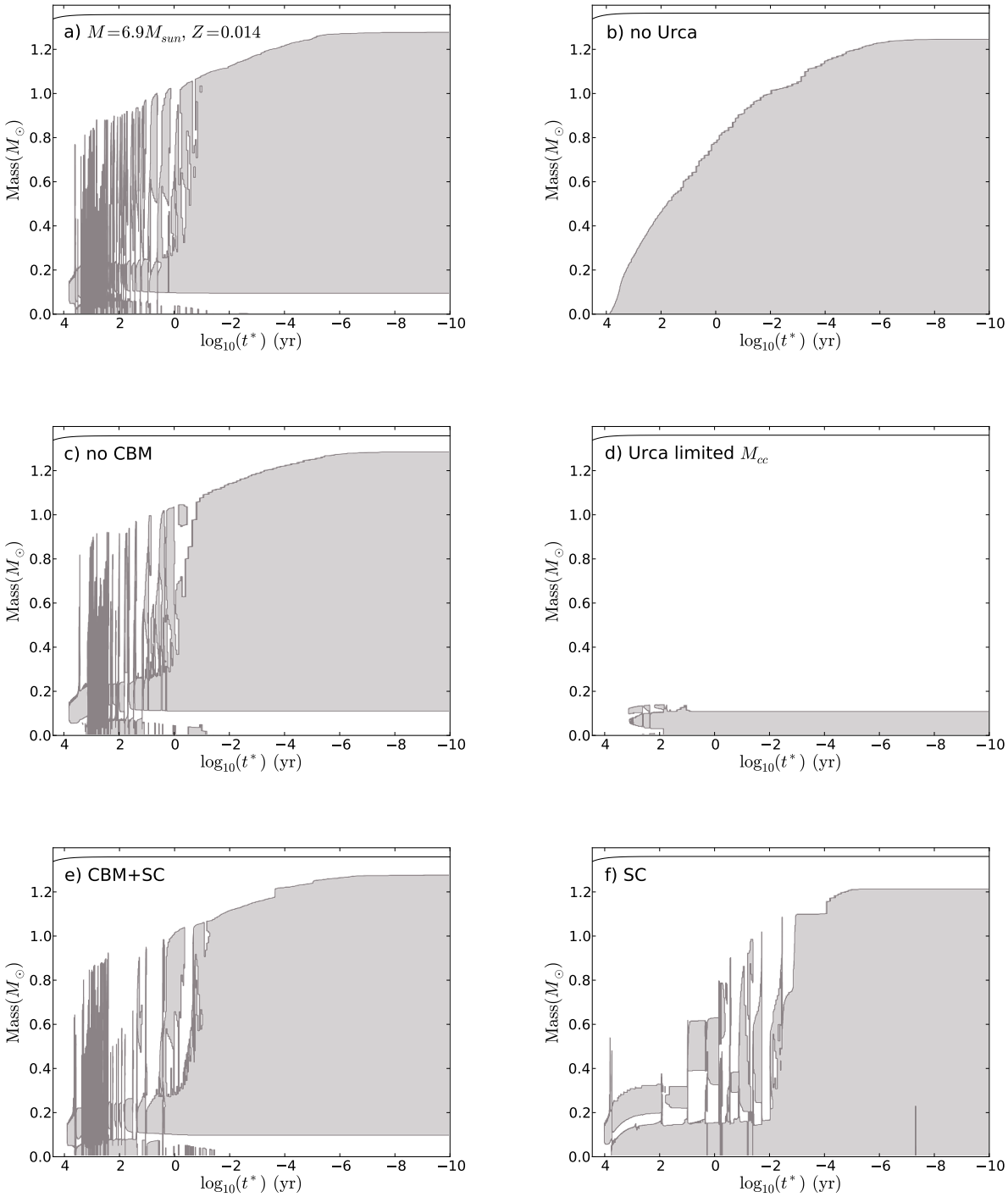

Figure 9. Kippenhahn diagrams for the hybrid C-O-Ne white dwarf with $M_{\rm i} = 6.9\,M_\odot$ (the solid blue curve in Fig. 3) accreting C-rich material with the rate $8 \times 10^{-7}\,M_\odot\,{\rm yr}^{-1}$ when it approaches the phase of the explosive C ignition. The diagrams are shown for the different mixing assumptions that are discussed in the text. The grey shades show convective zones.

ited $M_{\rm cc}$" we again find an explosive C ignition off the centre (Fig. 9d and the solid red curve in Fig. 10).

4 DISCUSSION AND CONCLUSION

Denissenkov et al. (2013) and Chen et al. (2014) have proposed a new class of WD models, called "the hybrid C-O-Ne WDs" that consist of a CO core surrounded by a thick ONe zone. At their birth, they also have a thin CO-rich buffer

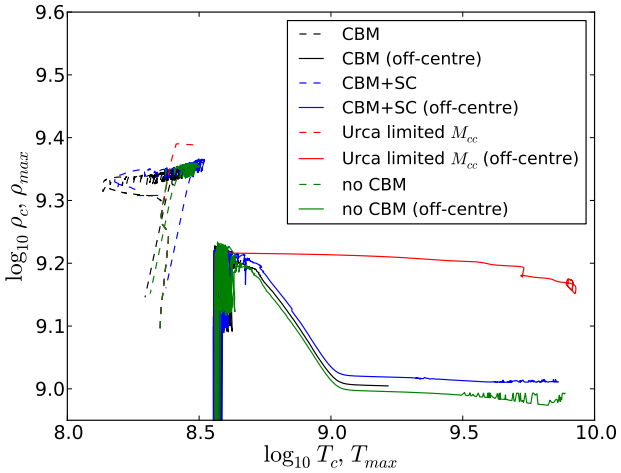

Figure 10. Same as in Fig. 6, but for the hybrid C-O-Ne white dwarf with $M_{\rm i} = 6.9\,M_\odot$ (the solid blue curve in Fig. 3) and for the mass accretion rate of $8 \times 10^{-7}\,M_\odot\,{\rm yr}^{-1}$. In these cases, the explosive C ignition occurs off the centre as a result of Urca cooling in the centre, therefore two sets of curves are shown, one for the centre (dashed curves) and the other for the point where the temperature has a maximum (solid curves).

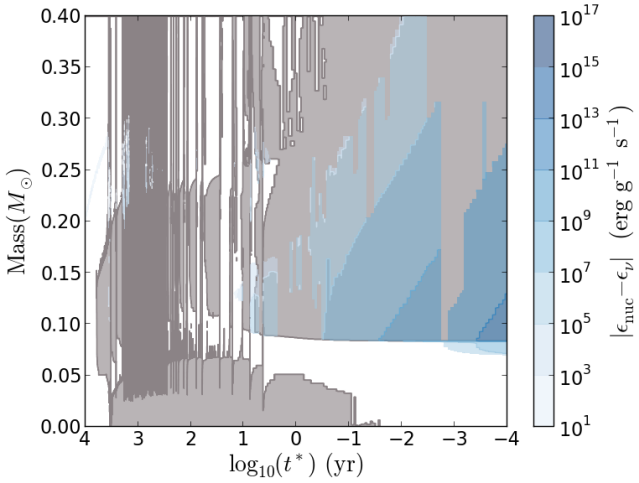

Figure 11. Zoomed in Kippenhahn diagram from Fig. 9a. The added shades of blue show the energy generation by the Urca reactions and C burning.

zone at the surface. Our stellar evolution calculations have shown that, when we include the observationally constrained extent of CBM outside the H and He convective cores, as modeled by equation (1) with $f = 0.014$, and assume that $f = 0.007$ outside the stiffer boundaries of the C convective zone in the core of a super-AGB star, the range of the initial mass of the stars with $Z = 0.014$ and $X = 0.70$ that give birth to the hybrid WDs is between $M_{\rm i} \approx 6.4\,M_\odot$ and $M_{\rm i} \approx 7.3\,M_\odot$ (Fig. 3). The aim of this work has been to find out if the hybrid WDs can be progenitors of SNe Ia, like their pure CO counterparts, provided that they are formed in binary systems with parameters suitable for the SD channel. To answer this question, we have allowed two of our hybrid WD models, those with $M_{\rm i} = 6.9\,M_\odot$ and $M_{\rm i} = 7.3\,M_\odot$, to accrete material with chemical composition identical to that of their surface layers until C is ignited explosively or it fails to do so. For the completeness of our study and for a comparison, we have also considered the evolution of the accreting CO WD with $M_{\rm i} = 6.3\,M_\odot$.

We have found that the most massive of our hybrid WD models, the one with $M_{\rm i} = 7.3\,M_\odot$ and, because of the similarity of their ^{12}C mass fraction profiles (the red and green curves in Fig. 3), also the model with $M_{\rm i} = 7.1\,M_\odot$, will probably experience an electron-capture induced collapse leading to an ECSN, when its mass approaches the Chandrasekhar limit. This happens with its slightly more massive pure ONe counterparts (Jones et al. 2013). This outcome is not surprising, given the small mass of the CO core in this star. The non-explosive C ignition in its centre leads to the development of a C convective core, in which the high C abundance from the CO core is diluted with the low C abundance in the ONe zone. As a result, the diluted C abundance turns out to be so low that the energy generated in the C burning is surpassed by the neutrino cooling and, after its initial attempt to go up, the central temperature begins to decline rapidly. The continuing increase of WD's mass and associated increase of its central density will eventually make electron-capture reactions efficient enough to induce a collapse of the star.

The hybrid WD model with $M_{\rm i} = 6.9\,M_\odot$ has quite a large CO core, so that even after the carbon from the CO core is mixed with what is left of it in the ONe zone the resulting C abundance still remains high enough for the C burning to successfully compete with the neutrino cooling. As a result, we find the explosive C ignition in all the substances of this WD model that we have obtained making different assumptions about mixing. The most difficult problem that we encounter in this model is the convective Urca process uncertainty. It has been known since the 1970s, but it is emphasized in our hybrid WD models because they have very high abundances of the Urca mother nuclei ^{25}Mg and, especially, ^{23}Na, the latter being one of the main products of C burning. The stellar evolution code of MESA that we use does account for the change of thermal energy produced by the Urca reactions because it includes terms similar to (5) in its energy equation. However, the MLTs of convection used in MESA do not take into account the extraction of kinetic energy from convective motion by the Urca processes, which is the major source of the Urca process uncertainty. Guided by the results of the 2D hydrodynamical simulations of Stein & Wheeler (2006) as well as by those obtained with the two-stream formalism by Lesaffre, Podsiadlowski & Tout (2005), and in the absence of reactive-convective 3D hydrodynamical simulations of the convective Urca process, we have chosen to consider a number of alternative instances of our accreting hybrid WD model for different mixing assumptions that are made to mimic the potentially possible outcomes of the interaction between convection and Urca reactions. These assumptions include the two limiting cases in one of which there are no Urca reactions at all ("no Urca"), while in the other Urca reactions completely suppress any mixing ("no mixing"). The mixing assumption suggested by the simulations of Stein & Wheeler (2006) is the "Urca limited $M_{\rm cc}$". It limits the size of the C convective core by the location of the ^{23}Na/^{23}Ne Urca shell. We have also added

the semiconvection. The T_c - ρ_c trajectories of the four model instances in which the explosive C ignition occurs off the centre are shown in Fig. 10, while the T_c - ρ_c trajectories of the three other model instances in which C explodes in the centre are shown in Fig. 8. Their corresponding Kippenhahn diagrams are gathered in Fig. 9.

From the presented results, we have come to the conclusion that the hybrid C-O-Ne WDs can be progenitors of SNe Ia, provided that the initial masses of their parent stars are between $M_i \approx 6.5\,M_\odot$ and $M_i \approx 6.9\,M_\odot$. However, their exact thermal and chemical structures at the moment of C explosion are uncertain and depend on the effects of the Urca processes on convective mixing. These effects are most likely to be strongly non-linear (e.g. Bisnovatyi-Kogan 2001), therefore we think that only future reactive-convective 3D hydrodynamical simulations will be able to estimate them quantitatively. We have generated several potentially possible instances of the hybrid SN Ia progenitor model that can be used, in the meanwhile, as initial models for 2D or 3D simulations of SN Ia explosion to see how their resulting nucleosynthesis yields and light curves differ from each other and if they match any of available SN Ia observations. The hybrid WDs should probably lead to SNe Ia that are different in some aspects from those produced from the pure CO WDs because they have much lower C/O abundance ratios and a slightly smaller electron-to-nucleon ratio Y_e, the latter being affected by the high ^{23}Na abundance (Timmes, Brown & Truran 2003). Accounting for their existence should also modify the predicted SN Ia and ECSN rates.

Although it can be expected that the less massive of our stars will enter a phase of explosive C-burning once their cores approach the Chandrasekhar mass, it is unlikely that the outcome will be a normal SN Ia. If the burning would proceed as a detonation from the start, the lack of intermediate-mass elements in the ejecta would, like in the pure CO white dwarfs, contradict observations. In contrast, a deflagration ignited in the CO core cannot change into a detonation in the ONe zone easily because the critical mass for a detonation of an O and Ne mixture is much larger than that of carbon. Therefore, the more likely outcome of such an explosion is a faint SN Ia, similar to the SN 2002cx class, as was also found for pure-deflagration CO white dwarfs, and possibly a bound remnant is left behind (Fink et al. 2014, and references therein).

Estimates of SNIa birthrates with our hybrid WD progenitors have recently been made by Meng & Podsiadlowski (2014) and Wang et al. (2014). They have found that these rates can range from a few to 18%, depending on the assumptions about the carbon burning rate, which is still very uncertain (Chen et al. 2014), chemical composition of the accreted material and details of the used binary population synthesis model.

ACKNOWLEDGMENTS

This research has been supported by the National Science Foundation under grants PHY 11-25915 and AST 11-09174. This project was also supported by JINA (NSF grant PHY 08-22648). Falk Herwig acknowledges funding from Natural Sciences and Engineering Research Council of Canada (NSERC) through a Discovery Grant. Pavel Denissenkov thanks Wolfgang Hillebrandt for his comments. Ken Nomoto acknowledges the support from the Grant-in-Aid for Scientific Research (23224004, 23540262, 26400222) from the Japan Society for the Promotion of Science, and the World Premier International Research Center Initiative (WPI Initiative), MEXT, Japan.

REFERENCES

Barkat Z., Wheeler J. C., 1990, ApJ, 355, 602
Becker S. A., Iben, Jr. I., 1979, ApJ, 232, 831
Bisnovatyi-Kogan G. S., 2001, MNRAS, 321, 315
Bours M. C. P., Toonen S., Nelemans G., 2013, A&A, 552, A24
Bruenn S. W., 1973, ApJ, 183, L125
Cassisi S., Iben, Jr. I., Tornambè A., 1998, ApJ, 496, 376
Chen M. C., Herwig F., Denissenkov P. A., Paxton B., 2014, MNRAS, 440, 1274
Chen X., Han Z., Meng X., 2014, MNRAS, 438, 3358
Couch R. G., Arnett W. D., 1975, ApJ, 196, 791
Denissenkov P. A., Herwig F., Truran J. W., Paxton B., 2013, ApJ, 772, 37
Denissenkov P. A. et al., 2014, MNRAS, 442, 2058
Fink M. et al., 2014, MNRAS, 438, 1762
Gamow G., Schoenberg M., 1941, Physical Review, 59, 539
Gehrz R. D., Truran J. W., Williams R. E., Starrfield S., 1998, PASP, 110, 3
Hachisu I., Kato M., Nomoto K., 1996, ApJ, 470, L97
Herwig F., Woodward P. R., Lin P.-H., Knox M., Fryer C., 2014, ApJ, 792, L3
Hillebrandt W., Niemeyer J. C., 2000, ARA&A, 38, 191
Iben, Jr. I., 1982, ApJ, 253, 248
Iben, Jr. I., Tutukov A. V., 1991, ApJ, 370, 615
Jones S. et al., 2013, ApJ, 772, 150
Langer N., El Eid M. F., Fricke K. J., 1985, A&A, 145, 179
Lesaffre P., Podsiadlowski P., Tout C. A., 2005, MNRAS, 356, 131
Ma X., Chen X., Chen H.-l., Denissenkov P. A., Han Z., 2013, ApJ, 778, L32
Meng X., Podsiadlowski P., 2014, ApJ, 789, L45
Mochkovitch R., 1996, A&A, 311, 152
Nomoto K., 1982a, ApJ, 257, 780
Nomoto K., 1982b, ApJ, 253, 798
Nomoto K., Saio H., Kato M., Hachisu I., 2007, ApJ, 663, 1269
Oda T., Hino M., Muto K., Takahara M., Sato K., 1994, Atomic Data and Nuclear Data Tables, 56, 231
Paczyński B., 1972, ApJ Lett., 11, 53
Paxton B., Bildsten L., Dotter A., Herwig F., Lesaffre P., Timmes F., 2011, ApJS, 192, 3
Paxton B. et al., 2013, ApJS, 208, 4
Perlmutter S. et al., 1999, ApJ, 517, 565
Phillips M. M., 1993, ApJ, 413, L105
Riess A. G. et al., 1998, AJ, 116, 1009
Shen K. J., Bildsten L., 2009, ApJ, 699, 1365
Stein J., Barkat Z., Wheeler J. C., 1999, ApJ, 523, 381
Stein J., Wheeler J. C., 2006, ApJ, 643, 1190
Tang S. et al., 2014, ApJ, 786, 61
Timmes F. X., Brown E. F., Truran J. W., 2003, ApJ, 590, L83

Toki H., Suzuki T., Nomoto K., Jones S., Hirschi R., 2013, Phys. Rev. C, 88, 015806
Wang B., Han Z., 2012, New A. Rev., 56, 122
Wang B., Meng X., Liu D.-D., Liu Z.-W., Han Z., 2014, ApJ, 794, L28
Weiss A., Hillebrandt W., Thomas H.-C., Ritter H., 2004, Cox and Giuli's Principles of Stellar Structure
Wolf W. M., Bildsten L., Brooks J., Paxton B., 2013, ApJ, 777, 136
Woosley S. E., Weaver T. A., 1994, ApJ, 423, 371